Supplementary Information for

Deconstructing the Enhancing Effect on CO_2 Activation in the Electric Double Layer with EVB

Xiaoyu Chen[1], Mårten. S. G.Ahlquist[1*]

[1]Division of Theoretical Chemistry&Biology, School of Engineering in Chemistry, Biotechnology and Health, KTH Royal Institute of Technology, 10691 Stockholm, Sweden

*E-mail: ahlqui@kth.se

Table of Contents

1. Computational Details

1.1. Quantum Mechanical Calculations

All DFT calculations for geometry optimisations and free energy estimations were carried out by Schrodinger's Jaguar 8.3 package[1]. The geometries of Co^{I}(TPP)----CO_2^- (reactant state) and Co(TPP)-CO_2^- (product state) were first optimised using Jaguar 8.3 at B3LYP-D3/LACVP** level of theory, high-level single point calculations were then performed at LACV3P**++/m06 level of theory on the optimised structures. Solvation energy estimations were done by using a dielectric continuum model with pre-calibrated parameters for different solvents as implemented in Jaguar. Frequency calculations were performed to confirm the optimised geometries were indeed minimal as well as to obtain thermodynamic data for Gibbs free energy calculations, which is defined as $G = E_{solv}$(B3LYP-D3/LACVP**) + ZPE(M06/LACV3P**++) + H_{298} - TS_{298} + 1.9 kcal/mol. The 1.9 kcal/mol is a concentration correction to the free energy of solvation, since the energy in Jaguar refers to the states 1M(g) to 1M(aq).

The transition state was located by relaxed coordinate scan and confirmed by the presence of one imaginary frequency. Its Gibbs free energy was then computed by the same formulism as above.

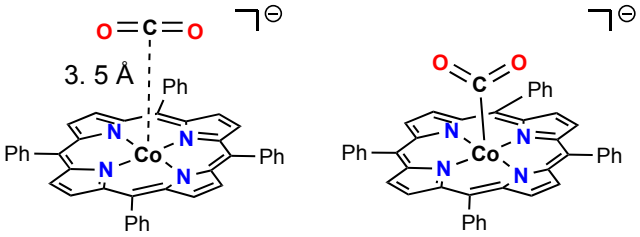

Figure S1. The structures for the reactant state (left) and product state(right)

1.2. Forcefield Parameterisation

Forcefield parameters, that are based on Amber's GAFF[2-3], were taken from a previous study on the Fe(porphyrin) unit in a heme system[4] while we calculated new atomic electrostatic potential (ESP) partial charges of the B3LYP-D3/LACVP** optimised structures by Jaguar 8.3. The equilibrium bond lengths, angles and dihedrals were taken from the above mentioned optimised structures. Parameters that were still missing (neither presented in GAFF nor in the Fe(porphyrin) paper mentioned above, i.e. N-Co-C-O dihedrals for Co(TPP)-CO_2^-) were fitted from the QM coordinate scan at 5° interval for 90° (that is, 18 data points in total) as oppose to 360° as a result of high symmetry. The newly constructed forcefield was then converted to GROMACS format by ACPYPE[5].

For the graphene sheet, the geometry was generated by the *genconf* command implemented in GROMACS while the topology file was created following Andrea Minoia's tutorial, which is published on GROMACS' official website (http://manual.gromacs.org/documentation/2019-rc1/how-to/special.html, access date: 23/06/2020), using OPLSA-AA force field. The short-range Lennard-Jones non-bonded interaction parameters were set to be the same as benzene carbons in OPLSA-AA (i.e. opls_145 in

GROMACS' notation). The partial charges for the carbon atoms were all set to zero as suggested by Andrea Minoia's tutorial.

1.3. Molecular Dynamics

All MD simulations were performed using GROMACS 2019.3 package[6-7]. The graphene sheet (36Å × 30 Å in size) was firstly minimised without position restrains in vacuum and then a 1ns simulation with timestep 0.002ps was performed first under NVT and thereafter under NPT to ensure its stability. In order to avoid self-interactions under periodic boundary conditions, a sufficient large box of 43.92 × 43.92 × 43.92 $Å^3$ was used for all simulations. In the next step, TIP3P water molecules were added and then the above steps were repeated to afford a relaxed graphene sheet with solvation.

The same preparations were done for the $Co^{I}(TPP)^-$ …. CO_2 as well as the $Co^{I}(TPP)^-$ …. CO_2 /graphene system. The treatment of other solvents (DMF, methanol) follows GROMACS' online tutorial (http://www.gromacs.org/Documentation/How-tos/Non-Water_Solvation, access date: 23/06/2020). Ions were added to the water-solvated system using the *genion* command implemented GROMACS and a salt concentration of 0.1M was selected, resulting in the addition of 4 K^+ and 4 Cl^- ions to the system. The resulted system was then relaxed in the same manner as described above.

When simulating the catalyst/graphene system, the graphene sheet was constrained with LINCs algorithm to mimic the fact that it was fixed on the electrode while the catalyst-CO_2 complex, ions and explicit solvent molecules, which filled the whole simulation box, were free to move.

1.4. Free Energy Pertubation(FEP)

The topology for FEP consists of the bonded state (i.e. product state, Co(TPP)-CO_2^-) and the non-bonded state (i.e. reactant state, $Co^{I}(TPP)$------CO_2). In specific, for the non-bonded state, the Co···CO_2 interaction was described in the [bond] section with a Morse potential fitted to Co···C Lennard-Jones 12-6 interactions.

```
[ bonds ]
; ai   aj   type
 33   35    3     0.202384    418.4   14.5          0.315   0.16     23.8
```

where 33 and 35 are the numbering for Co and CO_2 carbon atoms respectively. The number 3 under 'type' denotes Morse potential in GROMACS. The first set of parameters (red) describes the Co…CO_2 interaction in the bonded state, which is modelled by a Morse potential (as it converges to dissociation energy as oppose to plus infinity for a harmonic oscillator during the bond breaking process). The second set of parameters (blue) describes the Co…CO_2 interaction in the non-bonded state and was fitted Co···C Lennard-Jones 12-6 interactions.

In the [pairs] section, both Co···oxygen (oxygen of CO_2) pairs as well as N… carbon (carbon of CO_2) were added to describe the non-bonded interactions between them for both states. (For the full topology description, see **topol.top**)

```
[pairs]
  33   34    1   ; non-bonded interactions for Co – O (CO2)
  33   36    1   ; non-bonded interactions for Co – O (CO2)
   1   35    1   ; non-bonded interactions for N – C (CO2)
   8   35    1   ; non-bonded interactions for N – C (CO2)
  15   35    1   ; non-bonded interactions for N – C (CO2)
  22    35    1   ; non-bonded interactions for N – C (CO2)
```

N – oxygen (of CO_2) non-bonded interactions are already considered when GAFF based AMBER forcefield was converted to GROMACS by ACPYPE[5].

```
     [distance_restraints]
33   35   1   1   1  0.15  0.5 0.6  2
```

A weak distance restraint was added to ensure that CO_2 does not escape. This is a common practice in EVB and is encouraged by Q6[8], which is a software specially designed for FEP and EVB.

The free energy change of transforming the system from the reactant state to the product state is a function of a coupling parameter, lambda λ. Please refer to GROMACS' tutorial on FEP for details (http://www.gromacs.org/@api/deki/files/262/=gromacs-free-energy-tutorial.pdf, access date: 23/06/2020). 68 lambda values (0.0 0.01 0.02 … 0.2 0.225 0.25 … 0.8 0.81 0.82 0.83 … 1.0) were used to slowly moved the system from the bonded state to the non-bonded state.

Before the production run, the system at each lambda value was first minimised and then equilibrated for 50ps first under NVT and then NPT at 298K with a timestep of 0.001ps. A production simulation of 200 ps (with the exception of 1ns for DMF solvent) with timestep 0.001 ps was performed at every lambda value with the full environment. Then a *rerun* was performed on only the Co(TPP)-CO_2 system. Solvation energy obtained from the simulation with full environment was later added to the ground state potential surface obtained by *rerun* at each energy point to give a complete energy profile. In the mdp file, '*calc_lambda_neighbors'* was set to be -1 so that the energy difference between each lambda state and all the other states were calculated.

1.5 Radial Distribution Functions (RDFs)

RDFs were calculated with the presence of ions and the electric field at both the reactant state and the product state. At each state, a standard MD of 50 ns with time step 0.001ps was performed, with a total of 50000 data points collected (one point every 1000 steps). Note that due to the small number of cations (5) existed in the system, RDFs produced are not smooth even after very long simulations.

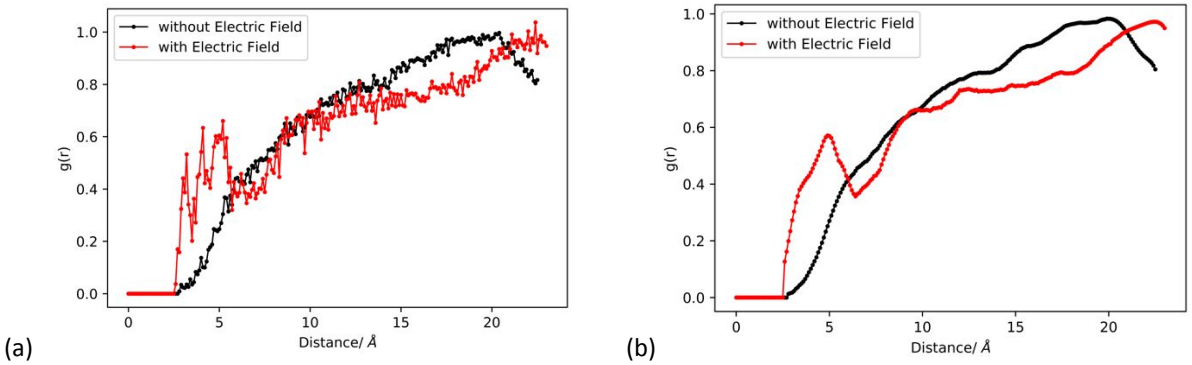

Figure S2. The RDFs for the reactant state: (a) plotted with original data. (b) smoothed curve produced after treated by a savitzky-golay filter.

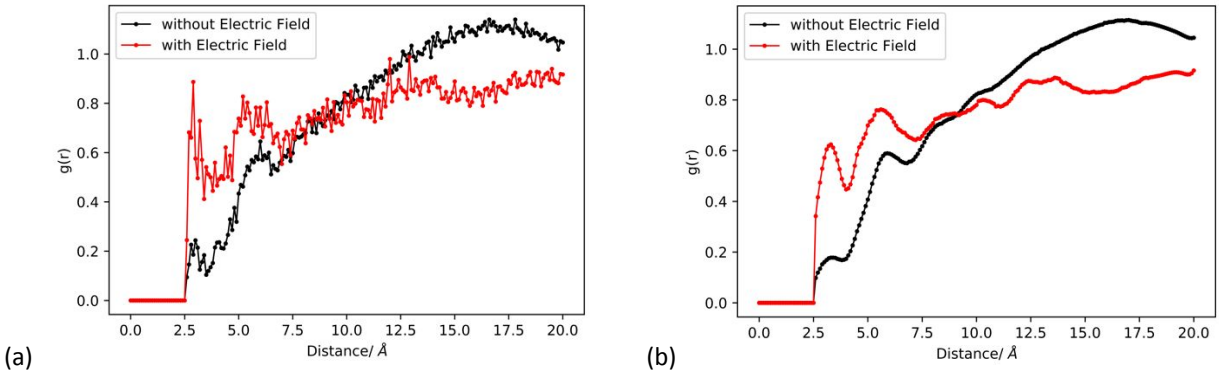

Figure S3. The RDFs for the reactant state: (a) plotted with original data. (b) smoothed curve produced after treated by a savitzky-golay filter.

2. Empirical Valence Bond (EVB)

2.1 Parameterisation

Empirical Valence Bond analysis takes the results from FEP calculations according to the method proposed by A. Warshel[9] in 1980s, where a chemical reaction is described by the linear combination of two VB states.

The Hamiltonians of the two VB states, say a reactant state (H1) and a product state (H2), are approximated by classical MD forcefields, with the exception of a Morse potential in place of the regular Harmonic potential to describe the bond to be broken/formed.

The reaction coordinate was described in term of the energy difference between the two states, say the reactant state (H1) and the product state (H2). In such a way one can describe the activation free energy, which reflects the probability of being at the transition state, on the ground-state potential surface (instead of as function of λ).

The ground state potential surface (E) can be obtained by solving the secular equation:

$$\begin{vmatrix} H1 - E & H_{12} \\ H_{21} & H2 - E \end{vmatrix} = 0 \qquad (1)$$

Where $H_{12} = H_{21.}$

Therefore, the ground state potential surface can be written as:

$$E = \frac{1}{2}(H1 + H2) - \frac{1}{2}\sqrt{(H1 - H2)^2 + 4H_{12}^2} \qquad (2)$$

Where H1 and H2 can be obtained from FEP calculation, H_{12} describes the coupling of the two states and is fitted empirically to DFT calculated value as explained in detail in section **1.1**. H_{12} was determined to be -8.0 kJ^2/mol^2 after fitting, which makes sense since relatively simple charge transfer processes are generally associated with small H_{12}.[9..]

The Gibbs free energy to move from the reactant state to the product state follows:

$$\Delta G(H1 \longrightarrow H2) = \sum_{m=0}^{n-1} \delta G(\lambda_m \rightarrow \lambda_{m+1}) = -\frac{1}{k_b T[<\exp(-k_b T(E - \varepsilon_m))>_m]} \qquad (3)$$

ε_m is the mapping potential that keeps the system around state X, which is described as:

$$\varepsilon_m = \lambda H1 + (1 - \lambda)H2 \qquad (4)$$

Obtaining ΔG as a function of λ is not sufficient to evaluate activation energy, which reflects the probability of being at the transition state on the ground state surface. The corresponding formulism defines the reaction coordinate as the energy difference between the reactant (H1) and product (H2) states. The free energy as a function of energy gap can be described as:

$$G(X) - \alpha = \Delta G(\lambda_m) - RT\,In < \delta(X' - X) \times e^{\frac{-E(X') - \varepsilon_m(X')}{RT}} >_m \qquad (3)$$

Where α is a constant describing the energy of formation, which is not covered in forcefield parameters; ΔG(X) is free energy as a function of reaction coordinate ; ΔG(λ) is free energy as a function of λ obtained from FEP calculation; m is a given FEP state; the delta function discretises the reaction coordinate X into finite intervals; E(X') is the ground state surface described in equation (2) ;
Since EVB is essentially a FEP process, in order to address complicated systems as the ones presented in this work, a python code was developed by our group to process the FEP data generated by GROMACS to create EVB profiles. Our python code together with one example is available at https://github.com/xyll313/EVB.

In order to calibrate the EVB model for our system (i.e. fit H_{12} and α), $G^{\ddagger}$ and ΔG from either high-level QM calculations or experimental data are required. In our case, $G^{\ddagger}$ and ΔG were calculated by QM as described in section **1.1.** The α and H_{12} value fitted for our system are -690.5 kJ/mol and 8.0 kJ^2/mol^2 respectively. Since EVB parameters are environment-independent[10], we were then able to use the fitted model to study the bond formation process in different, and rather complicated environment (e.g. different solvent, in the presence of a hydrophobic supporting material, electrolyte and/or an electric field) as explained in this work.

2.2 EVB Energy Profiles

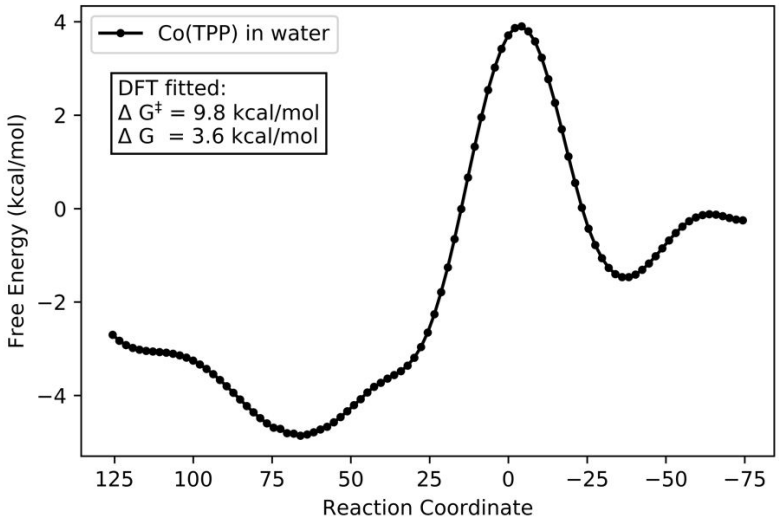

Figure S4. The EVB energy profile of CO_2 binding to a free $Co^{I}(TPP)^{-}$ in water fitted with DFT calculated activation energy ($\Delta G^{\ddagger}$) and reaction free energy (ΔG)

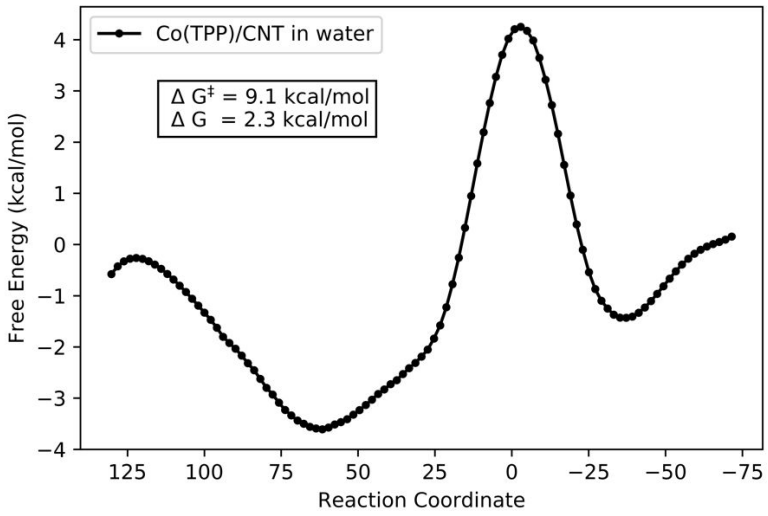

Figure S5. The EVB energy profile of CO_2 binding to the $Co^{I}(TPP)^{-}$/CNT system in water

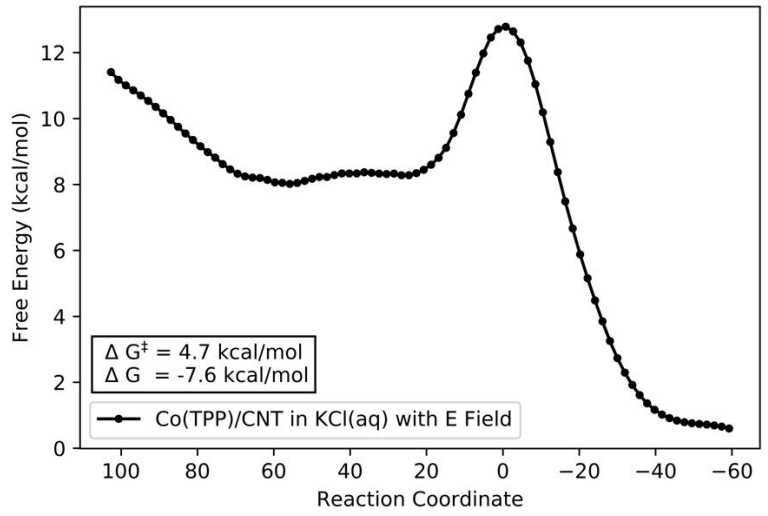

Figure S6. The EVB energy profile of CO_2 binding to the $Co^{I}(TPP)^{-}$/CNT system in 0.1 M KCl (aq) under an electric field strength of -0.4 V/m.

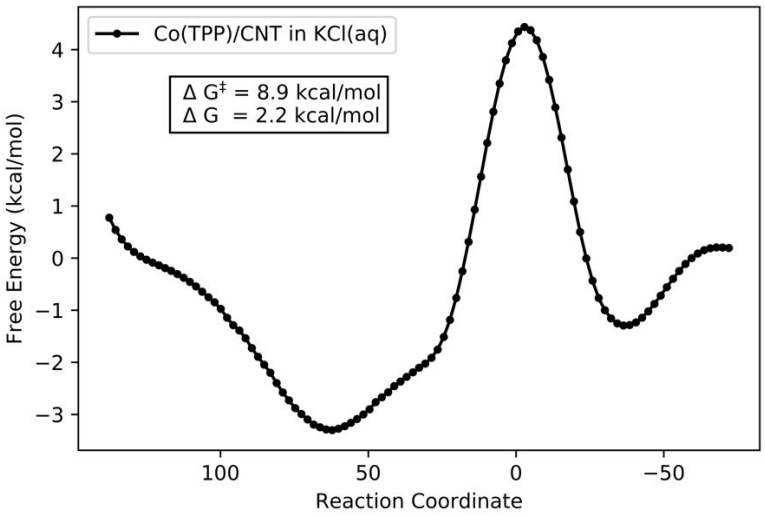

Figure S7. The EVB energy profile of CO_2 binding to the $Co^{I}(TPP)^{-}$/CNT system in 0.1 M KCl (aq)

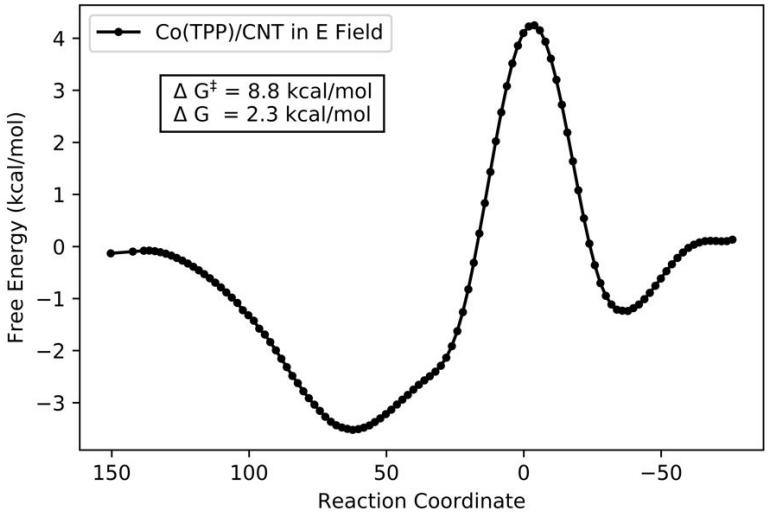

Figure S8. The EVB energy profile of CO_2 binding with to $Co^{I}(TPP)^{-}$/CNT system under an electric field of -0.4V/m.

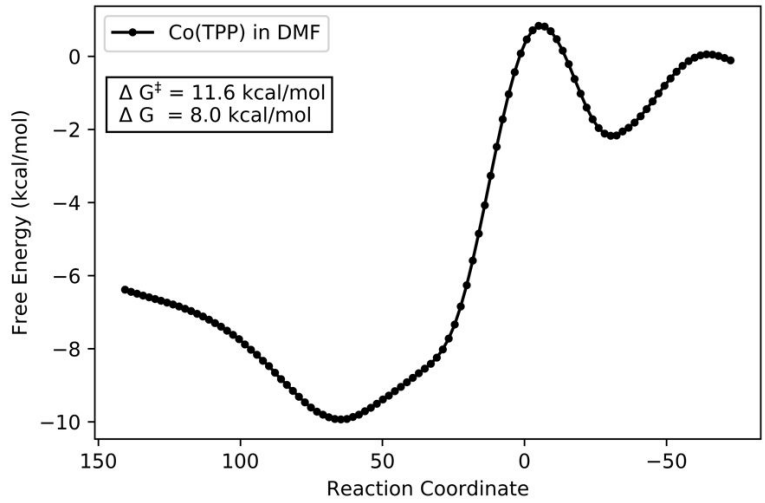

Figure S9. The EVB energy profile of CO_2 binding to a free $Co^{I}(TPP)^{-}$ in DMF

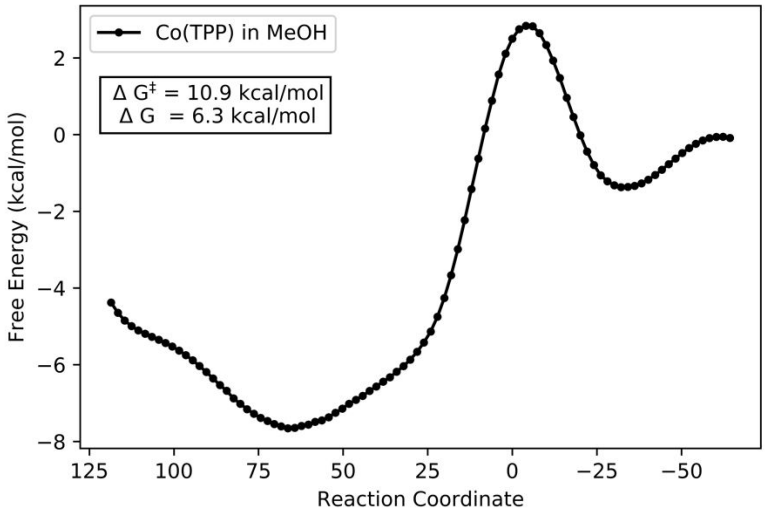

Figure S10. The EVB energy profile of CO_2 binding to a free $Co^{I}(TPP)^{-}$ in MeOH.

3. Results from Solvation Energy Analysis

Solvation energy at each lambda state was extracted by the 'gmx energy' command implemented in GROMACS. $Co^{I}(TPP)^{-}$ and CO_2 were defined in both *index* file and *mdp* option *energy_grps* in order to extract obtain their solvation energies separately. The same treatment was done for the $K^{+}\cdots CO_2$ interactions.

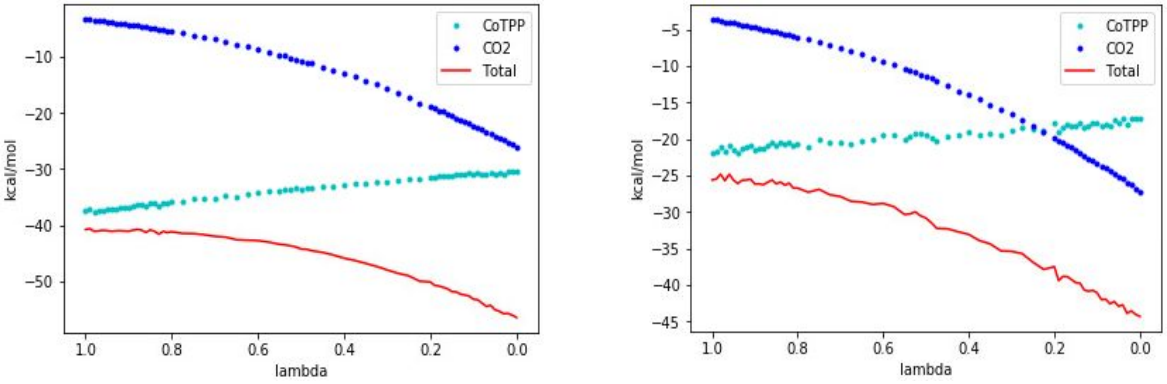

Figure S11. The change in solvation energy as a function of reaction coordinate (from unbonded $Co^{I}(TPP)^{-}\ldots CO_2$ state to bonded $[Co(TPP)\text{-}CO_2]^{-}$ state) for molecular $Co(TPP)^{-}$ in water(left) and $Co(TPP)^{-}$/graphene in water(right)

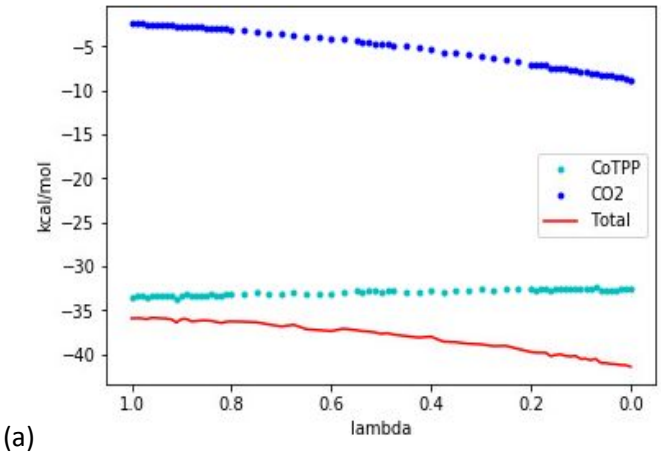

(a)

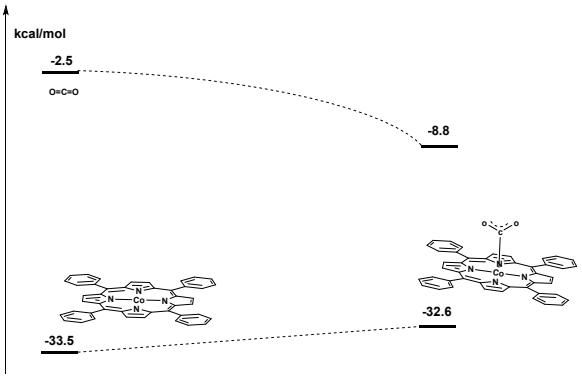

(b)

Figure S12. The change in solvation energy for molecular $Co(TPP)^-$ in DMF (a) as a function of reaction coordinate lambda (from unbonded $Co^I(TPP)^-…CO_2$ state to bonded $[Co(TPP)-CO_2]^-$ state); (b) as a chemdraw illustration

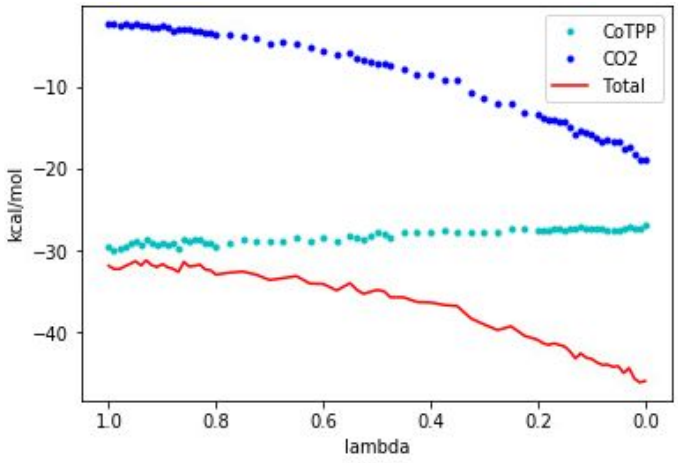

(a)

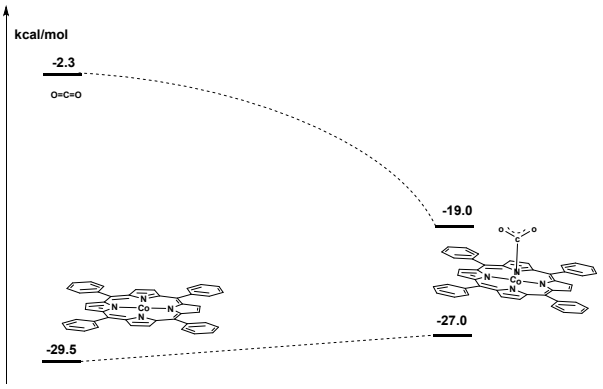

(b)

Figure S13. The change in solvation energy (a) as a function of reaction coordinate lambda for molecular $Co(TPP)^-$ in MeOH (from unbonded $Co^I(TPP)^-\ldots CO_2$ state to bonded $[Co(TPP)\text{-}CO_2]^-$ state) (b) as a chemdraw illustration

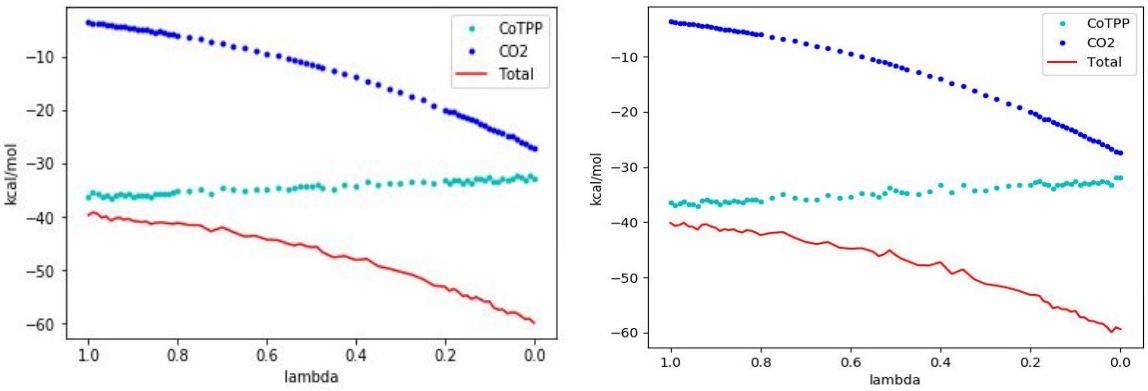

Figure S14 The change in solvation energy as a function of reaction coordinate (from unbonded $Co^{I}(TPP)^{-}$…CO_2 state to bonded $[Co(TPP)\text{-}CO_2]^{-}$ state) for $Co(TPP)^{-}$/graphene in KCl(aq) with (left) and without (right) an applied electric field of -0.4V/nm

4. Cation Distributions

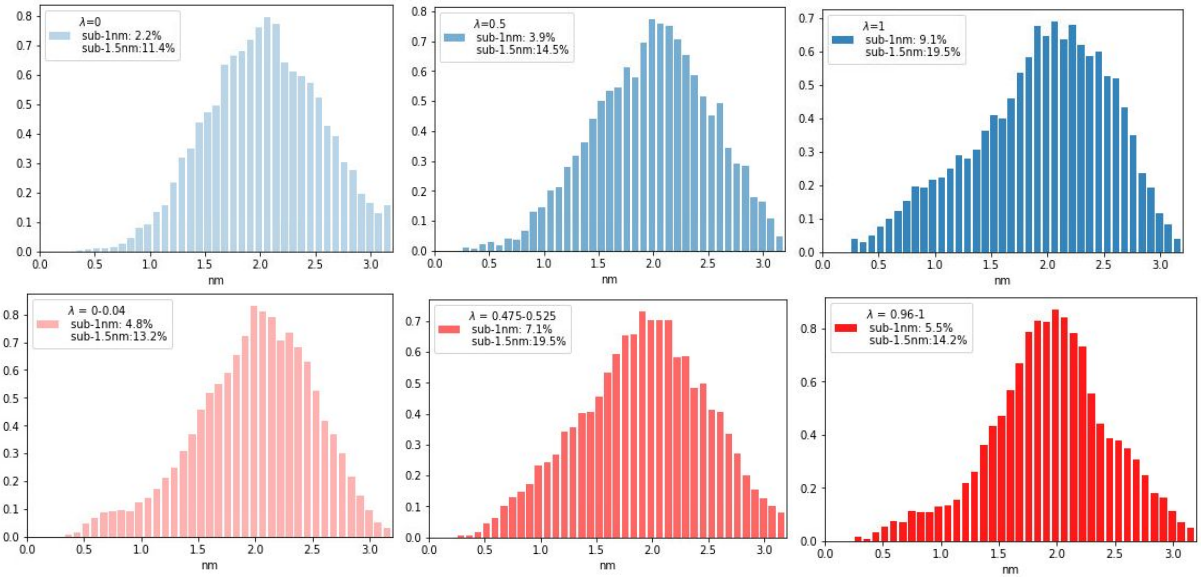

Figure S15. The distribution of K^+…CO_2 oxygen distances as a function of reaction coordinate lambda λ, with (blue) and without an applied electric field (red)

5. References

1. Bochevarov, A. D.; Harder, E.; Hughes, T. F.; Greenwoo, J. R.; Braden, D. A.; Philipp, D. M.; Rinaldo, D.; Halls, M. D.; Zhang, J.; Friesner, R. A., Jaguar: A High-Performance Quantum Chemistry Software Program with Strengths in Life and Materials Sciences. *Int. J. Quantum. Chem.* **2013**, *113*, 2010-2121.
2. Wang, J.; Wang, W.; A., K. P.; Case, D. A., Automatic Atom Type and Bond Type Perception in Molecular Mechanical Calculations. *J. Mol. Graph. Model.* **2006**, *25*, 247260.
3. Wang, J.; Wolf, R. M.; Caldwell, J. W.; Kollman, P. A.; Case, D. A., Development and Testing of a General Amber Force Field *J. Compt. Chem.* **2004**, *25*, 1157-1174.
4. Shahrokh, K.; Orendt, A.; Yost, G. S.; Cheatham III, T. E., Quantum Mechanically Derived Amber-Compatible Heme Parameters for Various States of the Cytochrome P450 Catalytic Cycle. *J. Comput. Chem.* **2012**, *33*, 119-133.
5. Sousa da Silva, A. W.; Vranken, W. F., Antechamber Python Parser Interface. *BMC Res Notes* **2012**, *5*.
6. Berendsen, H. J.; van der Spoel, D.; van Drunen, R., Gromacs: A Message-Passing Parallel Molecular Dynamics Implementation. *Comput. Phys. Commun.* **1995**, *91*, 43-56.
7. Abraham, M. J.; Van Der Spoel, D.; Lindahl, E.; Hess, B.; Team, G. D. *Gromacs User Manual Version 2019*, 2019.
8. Bauer, P.; Barrozo, A.; Purg, M.; Amrein, B. A.; Esguerra, M.; Wilson, P. B.; Major, D. T.; Åqvist, J.; Kamerlin, S. C. L., Q6: A Comprehensive Toolkit for Empirical Valence Bond and Related Free Energy Calculations. *Software X* **2018**, *7*, 388-395.
9. Hwang, J.-K.; King, G.; Creighton, S.; Warshel, A., Simulation of Free Energy Relationships and Dynamics of Sn_2 Reactions in Aqueous Solutions. *J. Am. Chem. Soc.* **1987**, *110*, 5297-5311.
10. Hong, G.; Rosta, E.; Warshel, A., Using the Constrained Dft Approach in Generating Diabatic Surfaces and Off Diagonal Empirical Valence Bond Terms for Modelling Reactions in Codensed Phases. *J. Phys. Chem. B.* **2006**, *110*, 19570-19574.